ISSN 0036-0295, Russian Metallurgy (Metally), Vol. 2006, No. 1, pp. 25–32. © Pleiades Publishing, Inc., 2006.
Original Russian Text © Ya.E. Beygelzimer, O.V. Prokof'eva, V.N. Varyukhin, 2006, published in Metally, 2006, No. 1, pp. 30–38.

Structural Changes in Metals Subjected to Direct or Twist Extrusion: Mathematical Simulation

Ya. E. Beygelzimer, O. V. Prokof'eva, and V. N. Varyukhin

Donetsk Physics and Technical Institute, National Academy of Sciences of Ukraine, Donetsk, 340114 Ukraine

e-mail: tean@an.dn.ua

Received November 30, 2004

Abstract—The structural evolution of a material is calculated using a phenomenological grain-refinement and failure model based on the relation between these two processes. Direct extrusion and various schemes of twist extrusion are compared, and the effect of pressure is considered. The results obtained are used to draw conclusions regarding the advantages of certain deformation schemes.

PACS numbers: 81.20.Hy, 61.43.Bn

DOI: 10.1134/S0036029506010058

INTRODUCTION

Technologies intended for the production of fine-grained materials via severe plastic deformation (SPD) are being actively developed [1]. Therefore, the possibility of prediction of the structural characteristics of a material produced by an SPD method is of great practical importance. A tool to obtain such information is mathematical simulation, since it allows one to choose optimum deformation schemes that provide the required set of properties of the end product, to calculate the time to failure for a blank in a certain process, and to trace the evolution of the structural characteristics of a material.

The classical model of the theory of plasticity [2] and the generally accepted fracture models of [3–5] cannot be used for these purposes, since they do not take into account a number of SPD effects. In particular, they cannot describe deformation localization in bands followed by the formation of void layer bands in deformed blanks that were observed in equal-channel angular pressing (ECAP) experiments.

To obtain adequate results when simulating SPD processes, one should take into account the relation between the processes of grain refinement and void formation. In this work, we present calculations performed in terms of the continuum model of grain refinement and failure during plastic deformation of a polycrystal [6] that is based on the principle of complementarity of these processes (namely, a decrease in the intensity of one of them cause an increase in the intensity of the other and vice versa). Using the results obtained, we draw certain conclusions regarding the advantages of a certain deformation scheme and formulate some recommendations concerning its realization.

SIMULATION BACKGROUND

The proposed description of the structural evolution of a material during plastic deformation is based on some assumptions and hypotheses, which are substantiated using the following physical data.

Several elementary deformation mechanisms are realized in polycrystalline materials (dislocation slip, dislocation cross slip, dislocation climb, twinning); each of them has a specific activation energy and provides a certain deformation rate under the given parameters of an external action (such as the stress, the strain rate, and the temperature). Under certain deformation conditions, operating mechanisms are the mechanisms that ensure the maximum deformation rate, i.e., the maximum decrease in the applied load [7].

During deformation, shears are known to be blocked inside structural elements; as a result, internal microstresses, which are the main cause of strain hardening at relatively low plastic strains, increase. These stresses are substantially inhomogeneous and cause bending and torsion of a crystal lattice; as a result, lattice regions in which dislocation charges accumulate (so-called accumulation zones (AZs)) form during plastic deformation [6]. In terms of our model, we assume that these zones can relax in two ways: via either the relative rotation of individual elements in the crystal lattice and, thus, the formation of the nucleus of a high-angle grain boundary or via the formation of a microvoid with a cross-sectional dimension of about 100 nm. The former way leads to grain refinement and the related hardening of the material, and the latter way leads to an increase in the damage to the material and a decrease in its plasticity. The probabilities of these mechanisms of stress relaxation are determined by the properties of the material, the pressure, the temperature, and the strain rate.

Microvoids do not change their dimensions during deformation, and the failure of a material consists in their gradual accumulation to a certain concentration (about 0.01 of the material volume), which is taken to be the criterion of macroscopic failure during plastic deformation [8].

After [9, 10], we suppose that the transformation of a crystal structure caused by the appearance of a microvoid or a high-angle-boundary nucleus proceeds much faster than deformation. The other relaxation processes have no time to occur during deformation. This assumption is justified for cold plastic deformation.

In our model, we introduce two scalar parameters characterizing a material structure to describe the grain refinement and failure of metallic materials. The parameter that reflects the development of a network of high-angle grain boundaries is taken to be their total length S per unit cross-sectional area of the representative material volume. The quantitative measure of failure of the representative volume is the total void volume Θ per unit material volume.

Each fragment consists of a group of cells surrounded by high-angle grain boundaries. Cell boundaries form a fine network with a grain size of d_c along which high-angle grain boundaries propagate [10]. This means that d_c represents the minimum size of a high-angle grain boundary section or the minimum fragment size. This parameter is specified by the material composition, the temperature, and the strain rate and is independent of the initial structure of the material and the type of loading. To estimate the cell size, we use the experimental data of [10], where d_c in metals was shown to be $d_c \approx 100$ nm.

It is natural to assume that grain refinement proceeds in several stages. As long as the fragment size is much larger than a certain critical radius of bending resulting in a new boundary, the physical mechanism of structure grain refinement is independent of the fragment size. Here, $S_0 \ll S \ll S_c \approx d_c^{-1}$, where S_0 is the initial length of high-angle grain boundaries per unit cross-sectional area (grain-boundary length). As soon as the fragment size is on the order of the critical bending radius (which corresponds to the case $S \longrightarrow S_c$), further division terminates due to the fact that the bending or rotation of such small fragments requires extremely high stresses. The sliding of some individual fragments with respect to the others becomes energetically favorable. The termination of grain refinement results in the fact that, at high strains, the sizes of all fragments become equal to the minimum possible size d_c. During further deformation, the fragment size remains unchanged and internal stresses do not increase, since they relax upon fragment sliding. Moreover, dynamic equilibrium between the processes of microdiscontinuity formation and healing is established.

CONTINUUM MODEL OF GRAIN REFINEMENT AND FAILURE IN A POLYCRYSTAL

We consider the plane section of the representative volume of a polycrystal. Then, an AZ, a grain-boundary nucleus, and a microvoid in this section correspond to points, since the characteristic size of the representative volume is much larger than the characteristic sizes of these objects. Let N and N_b be the numbers of AZs and boundary nuclei per unit cross-sectional area of the polycrystal, respectively. Then, we obtain kinetic equations for N, N_b, S, and Θ (they were derived in [6]).

In the grain refinement stage where the law of grain refinement is still independent of the fragment size, a so-called self-similar process appears. This means that, beginning from a certain loading time, any crystal region is a scaled-down copy of the entire crystal. After [11], if the sequential division of any object into parts is self-similar (i.e., if the law according to which a large object is divided into small parts is independent of its size), the size distribution of fragments becomes lognormal during this process. Fragments that are not subjected to division (i.e., their size has reached d_c) appear during deformation; however, we can neglect their fraction at the self-similar stage. Their number then increases, and the size distribution of fragments ceases to be lognormal.

This circumstance is taken into account in the model by introducing a factor $F(S)$, which represents the fraction of fragments undergoing division during plastic deformation; then, $(1 - F(S))$ is the fraction of undivided fragments. Thus, $F(S) = 1$ at $S_0 \ll S \ll S_c \approx d_c^{-1}$, and this factor vanishes at $S \longrightarrow S_c$.

For the number of AZs, we have

$$dN = \left(\frac{C_1}{\Delta^2} + C_2(S_0 + S)\frac{dS}{d\gamma}\right)F(S)d\gamma - (C_3(p) + C_4)Nd\gamma, \quad (1)$$

where Δ is the characteristic structural size corresponding to d_c; C_1 and C_2 are the parameters that are responsible for the number of obstacles to boundary shear in the initial structure and for the number of deformation-induced obstacles, respectively,

$$C_3(p) = \frac{1}{\gamma_p(P)}, \quad C_4 = \frac{1}{\gamma_b}. \quad (2)$$

In the expression for C_3, the parameter $\gamma_p(P)$ is the threshold (quasimonotonic) strain at which the porosity of the material begins to increase sharply at a given pressure. In Fig. 1, which illustrates the physical meaning of $\gamma_p(P)$, this parameter corresponds to the strain at which a curve detaches from the abscissa axis. The argument P indicates that γ_p increases with the hydrostatic pressure in the representative volume of the material (we will discuss the explicit form of this dependence below).

In the expression for C_4, the parameter γ_b is the threshold strain at which high-angle grain boundaries begin to nucleate. The meaning of this parameter can be understood from Fig. 2, where it corresponds to the value of strain e at which S becomes nonzero (i.e., this is the first point in the curve). According to [13], $\gamma_b \approx 0.4$ for shear deformation. Thus, beginning from a strain of about 20%, one should expect the appearance of the first mesodefects in the form of broken boundaries in the structure of deformed samples.

The first term in Eq. (1) is responsible for the nucleation of AZs. The presence of the factor $F(S)$ indicates that, beginning from a certain strain, the rate of formation of these zones begins to decrease ($F(S) < 1$), since internal stresses are accumulated insignificantly because of the appearing possibility of relaxation via the sliding of some fragments with respect to others. At $S = S_c$, $F(S)$ makes this term zero. The second term in Eq. (1) corresponds to the "death" of AZs due to the formation of either microvoids or high-angle grain boundaries.

The nuclei of high-angle grain boundaries are mobile stress concentrators; when moving in a material during deformation, they leave behind them a deformation-induced boundary. When reaching such a boundary or a grain boundary, the mobile stress concentrators "die." Therefore, their mean free path is on the order of the mesh of the network formed by high-angle grain boundaries, $L \approx 1/(S + S_0)$. As follows from the assumption of the self-similarity of an ensemble of boundaries at various instants of time, the distance traveled by all concentrators is equal to

$$dl = C_5 L d\gamma, \tag{3}$$

where C_5 is a constant. Then, we can write the following differential equation for S:

$$dS = \frac{C_5 N_b d\gamma}{S + S_0}.$$

A change in the porosity of the material Θ during plastic deformation is caused by the processes of microvoid generation and healing, which is reflected by the differential equation

$$d\Theta = C_3(\bar{N}d_c^2)^{1.5}\nu d\gamma - C_6\Theta d\gamma, \tag{4}$$

where ν is the microvoid volume and

$$C_6 = 6aP/K. \tag{5}$$

In Eq. (5) for C_6, a is the parameter characterizing the morphology of pores and P/K is the rigidity of the state of stress with the sign reversed.

The minuend in Eq. (4) describes pore generation, and the subtrahend reflects the processes of microvoid healing during metal deformation under pressure and takes into account the fact that the intensity of this process is proportional to the porosity [8].

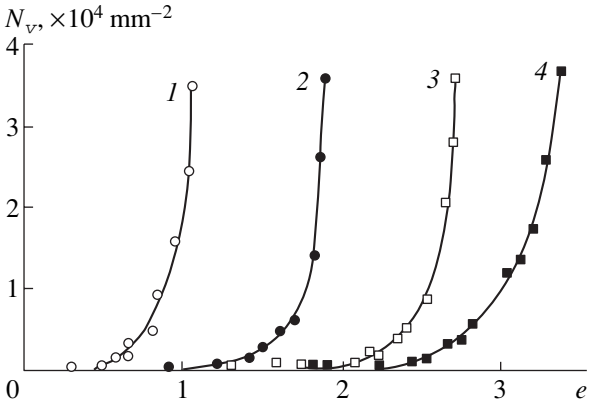

Fig. 1. Variation of the void density N_v with the strain e in grade 1045 steel samples [12] under a pressure of (*1*) 0.1 (atmosphere pressure), (*2*) 420, (*3*) 840, and (*4*) 1120 MPa. The upper points in the curves correspond to the appearance of a macrocrack.

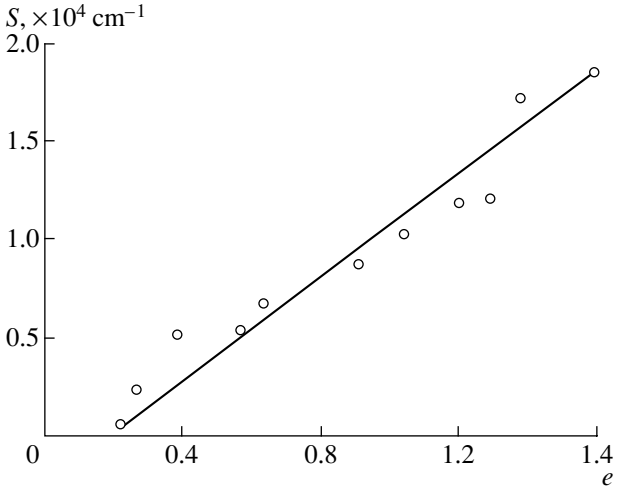

Fig. 2. Dependence of the total length S of deformation-induced boundaries in the unit area of a nickel polished section on the strain e [13].

By adding an equation for the number of high-angle-boundary nuclei N_b, we obtain a closed system of differential equations to describe grain refinement and failure during plastic deformation under pressure:

$$\begin{gathered}\frac{d\bar{N}}{d\gamma} = (C_1 + C_2C_5\bar{N}_b)F(\bar{S}) - (C_3 + C_4)\bar{N}, \\ \frac{d\bar{N}_b}{d\gamma} = C_4\bar{N} - C_5\bar{N}_b, \\ \frac{d\bar{S}}{d\gamma} = \frac{C_5\bar{N}_b}{\bar{S} + \bar{S}_0}, \\ \frac{d\Theta}{d\gamma} = C_3\bar{N}^{1.5}d_c^{-3}\nu - C_6\Theta.\end{gathered} \tag{6}$$

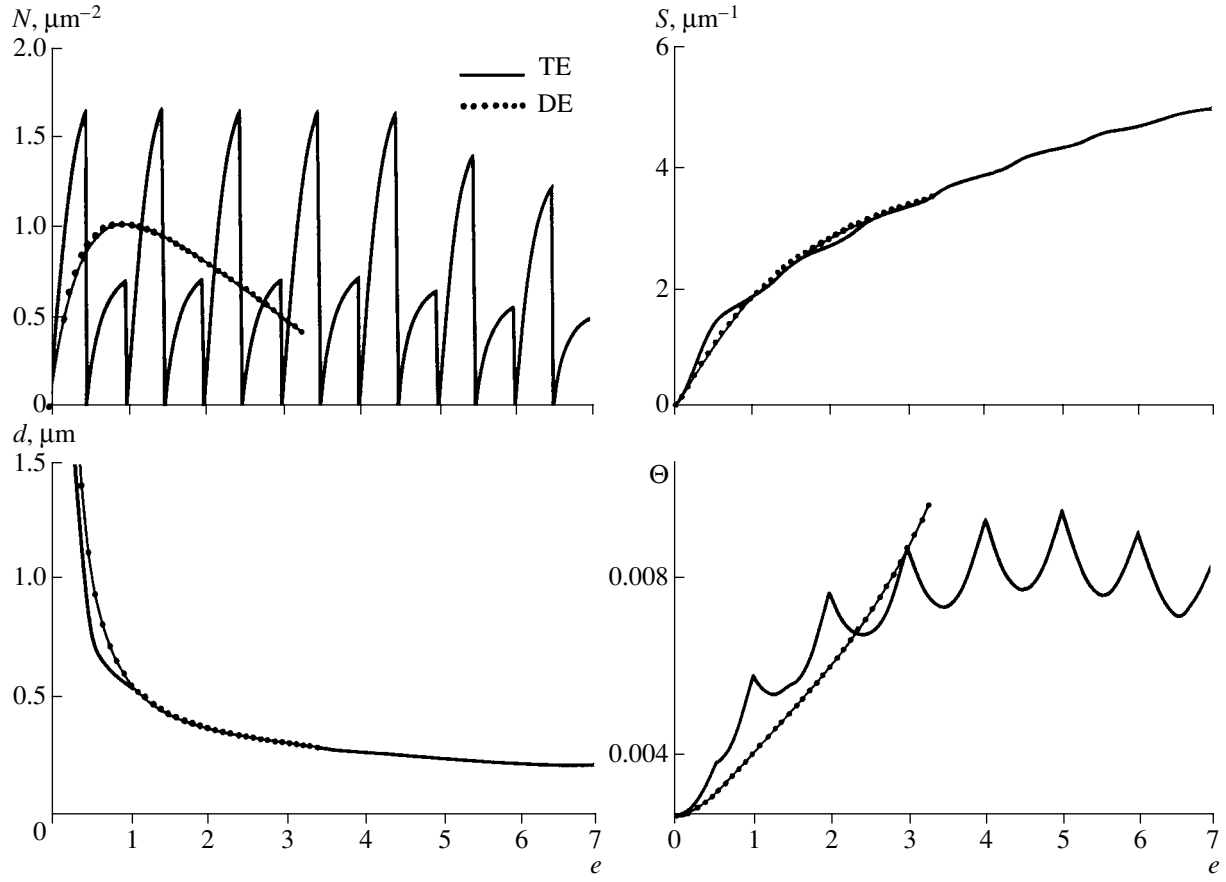

Fig. 3. Comparison of the structural characteristics of grade 45 steel for TE (seven sequential twist dies) and DE (three passes with an elongation $\lambda = 3$ in each pass) processes.

This system is written using the following dimensionless functions:

$$\bar{N} = Nd_c^2 = \frac{N}{S_c^2}, \quad \bar{N}_b = N_b d_c^2 = \frac{N_b}{S_c^2},$$

$$\bar{S} = Sd_c = \frac{S}{S_c}, \quad \bar{S}_0 = S_0 d_c = \frac{S_0}{S_c}.$$

In the case of quasimonotonic loading, system (6) should be solved with the initial conditions $\bar{N} = 0$, $\bar{N}_b = 0$, $\bar{S} = 0$, and $\Theta = 0$ at $\gamma = 0$.

To describe substantially nonmonotonic loading, the entire deformation process should be divided into quasimonotonic stages, and system (6) should be separately solved for each of them. Initial conditions for $\bar{N}_b$, $\bar{S}$, and Θ at any stage (except for the first stage) are taken to be the values of these quantities calculated at the previous stage. An initial condition for $\bar{N}$ at any stage is taken to be $\bar{N} = 0$, which reflects the disappearance of AZs as the loading direction changes abruptly.

To analyze the solutions to system (6) for various deformation schemes, we explain the physical meaning of certain model parameters.

In [8], we developed a continuum model for metal failure during plastic deformation that was based on a kinetic equation for deformation-induced porosity and a metal failure criterion. This criterion implies that a macrocrack appears at a certain critical value of porosity Θ_c that is independent of both the type of material and the state-of-stress parameters. This criterion was proposed by Rybin [9], who experimentally showed that $\Theta_c \approx 0.01$. For metal plasticity Λ_p (which is the strain to failure at a constant value of P/K), we obtained the expression [8]

$$\Lambda_p = \frac{1}{3a(P/K)} \ln\left[1 + 3a\frac{P}{K}\frac{\Theta_c}{\alpha}\right], \qquad (7)$$

where α is the so-called accommodation parameter; it reflects the ability of some structural elements in the material to fit other elements during plastic deformation ($\alpha = 0$ corresponds to complete accommodation of structural elements).

Relation (7) allows us to determine the parameters α and a from the experimental dependences $\Lambda_p =$

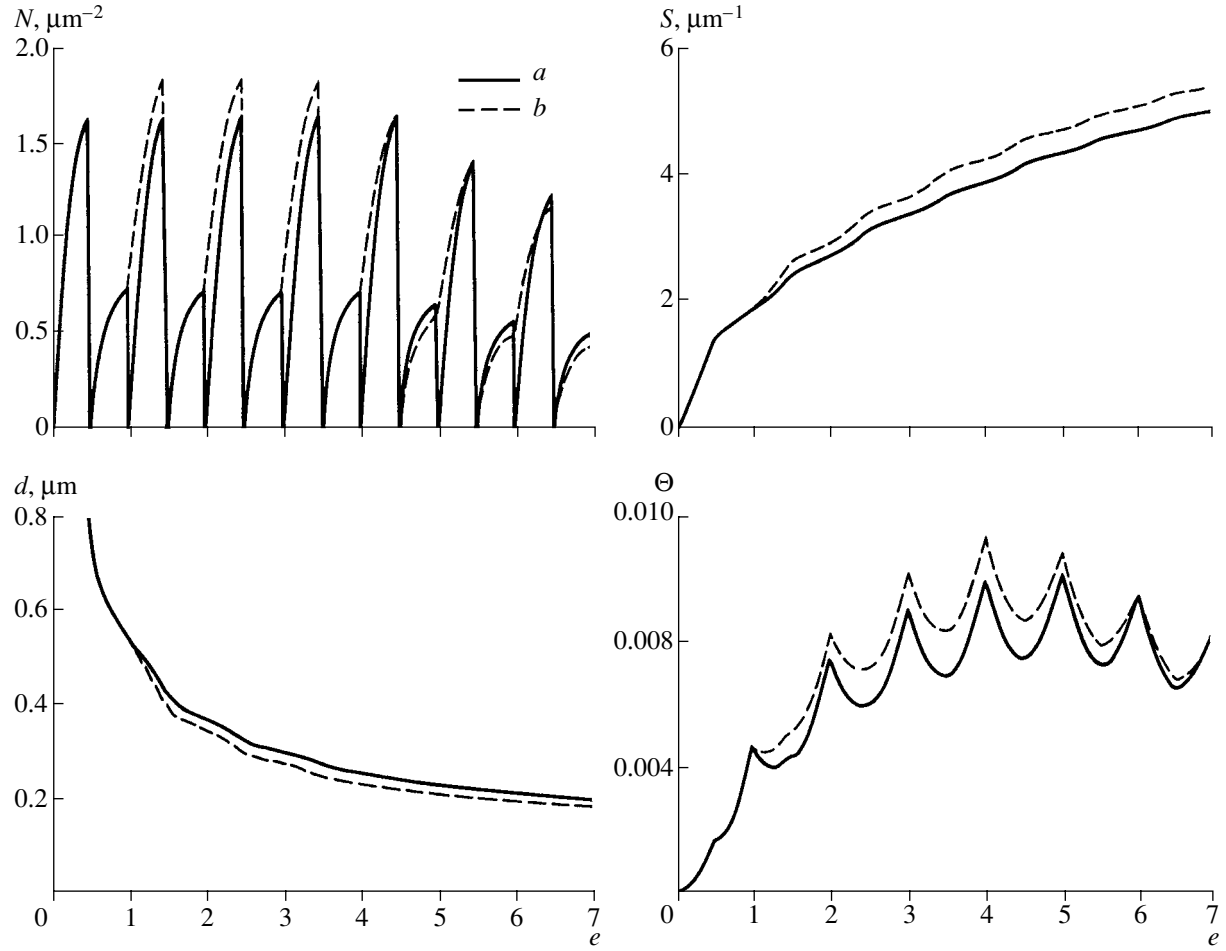

Fig. 4. Effect of cyclic deformation on the structural characteristics of grade 45 steel for two TE schemes: (*a*) seven sequential twist dies having the same orientation and (*b*) seven twist dies having alternating clockwise and counterclockwise orientations.

$\Lambda_p(P/K)$, i.e., from plasticity diagrams that are obtained from mechanical tests performed in testing machines that can realize various loading types (tension, compression, shear) at fixed values of P/K. From Eq. (7), we can write an expression for the parameter α:

$$\alpha = \Theta_c/\Lambda_{p0}, \tag{8}$$

where Λ_{p0} is the strain to failure at the zero value of the hydrostatic stress tensor component.

For the coefficient C_1, we can write

$$C_1 = (C_3 + C_4)\left(\frac{\alpha d_c^3}{C_3 \nu}\right)^{2/3}. \tag{9}$$

It follows from Eq. (8) that α is higher for the types of loading where plasticity is lower. Experiments demonstrate that plasticity diagrams depend substantially on the type of loading, and the value of $\Lambda_p(P/K)$ is usually minimum in simple-shear tests. Therefore, we can conclude that grain refinement is more intense in the deformation processes that result in a sharper decrease in the metal plasticity at the same level of hydrostatic pressure. However, to form submicro- and nanostructures, we have to realize these processes at a high hydrostatic pressure in the deformation zone. In this case, internal stresses relax via grain refinement rather than via microvoid formation. Thus, deformation based on simple shear under high pressure should be most effective to produce submicrostructures. This conclusion corresponds to the conclusions drawn experimentally in [14].

RESULTS OF SIMULATION OF SPECIFIC TREATMENT PROCESSES

We apply the model developed to describe twist (TE) and direct (DE) extrusion of grade 45 steel. Let us estimate the model parameters in an order of magnitude.

From structural analysis, we have $C_2 \approx 0.1$. For estimation, we assume that a high-angle-boundary nucleus travels the mean free path at a strain of about 0.1; then, from Eq. (3) we have $C_5 \approx 10$. The parameters γ_b and $\gamma_p(P)$ are estimated from the results shown in Figs. 1

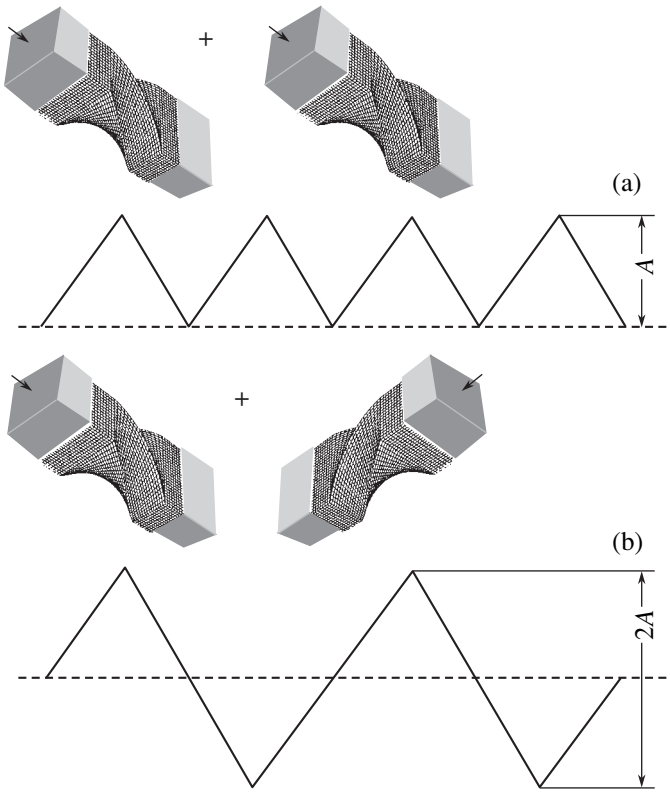

Fig. 5. Difference in the deformation amplitudes in the case of (a) like orientations and (b) alternating unlike orientations of twist dies.

and 2 because of the absence of the required data for grade 45 steel. As shown above, $\gamma_b \approx 0.4$; then, from Eq. (2), we obtain $C_4 \approx 2.5$. To determine the $\gamma_p(P)$ dependence, we first use Fig. 1 and obtain the pressure dependence of the strain corresponding to the onset of void formation (P was preliminarily normalized by K, which is the shear yield point of the material). By approximating this dependence by a straight line, we obtain the $\gamma_p(P)$ dependence in the explicit form

$$\gamma_p(P) = 0.3219 + 0.3874P/K.$$

Then, according to Eq. (2), we have $C_3 = (0.3219 + 0.3874P/K)^{-1}$.

Using the analytical expression $P/K = -\sigma/T$, we chose a deformation scheme in the framework of the model. The parameter P/K is constant only in the simplest cases, e.g., in upsetting or uniaxial tension. In particular, for DE, we have [15]

$$\frac{P}{K} = \sqrt{3}\ln\lambda - e + \frac{2}{\sqrt{3}},$$

where λ is the elongation and e is the logarithmic strain.

To a first approximation for TE, we specify the distribution of the state of stress along a die [16] so that

$$\frac{P}{K} = \frac{3}{4}\tan\beta + \frac{2fh}{r\cos\beta}, \quad 0 < z < h/2,$$
$$\frac{P}{K} = 0, \quad h/2 < z < h, \tag{10}$$

where β is the angle of die inclination, f is the coefficient of plastic friction, r is the twist-channel radius, h is the twist-channel height, and z is the coordinate along the channel. For the calculations given below, we use the following parameters: $\beta = 60°$, $f = 0.1$, $h = 20$ cm, and $r = 14$ cm. From Eq. (5), we obtain an expression for C_6 by making allowance for $a \approx 0.1$ [8].

As noted above, the plasticity curves depend on the type of loading, i.e., on the Lode coefficient μ_σ, which should be taken into account to determine α. In the case of tension ($\mu_\sigma = -1$), the plasticity curve is always located above the curve characteristic of pure shear ($\mu_\sigma = 0$). For DE, we have $\mu_\sigma = -1$ and, hence, $\alpha = 3.9 \times 10^{-3}$; for SE, $\mu_\sigma = 0$ and $\alpha = 5.4 \times 10^{-3}$.

We calculate C_1 using Eq. (9). The related quantities are estimated as follows: $d_c \approx 0.1$ μm [10] and $\nu \approx 0.005$ μm^3 [9].

Figure 3 shows the solutions to system (6) for TE and DE at the parameters given above. The curve of the average grain size d (which is reciprocal to S) is given for convenience, since this structural parameter is most

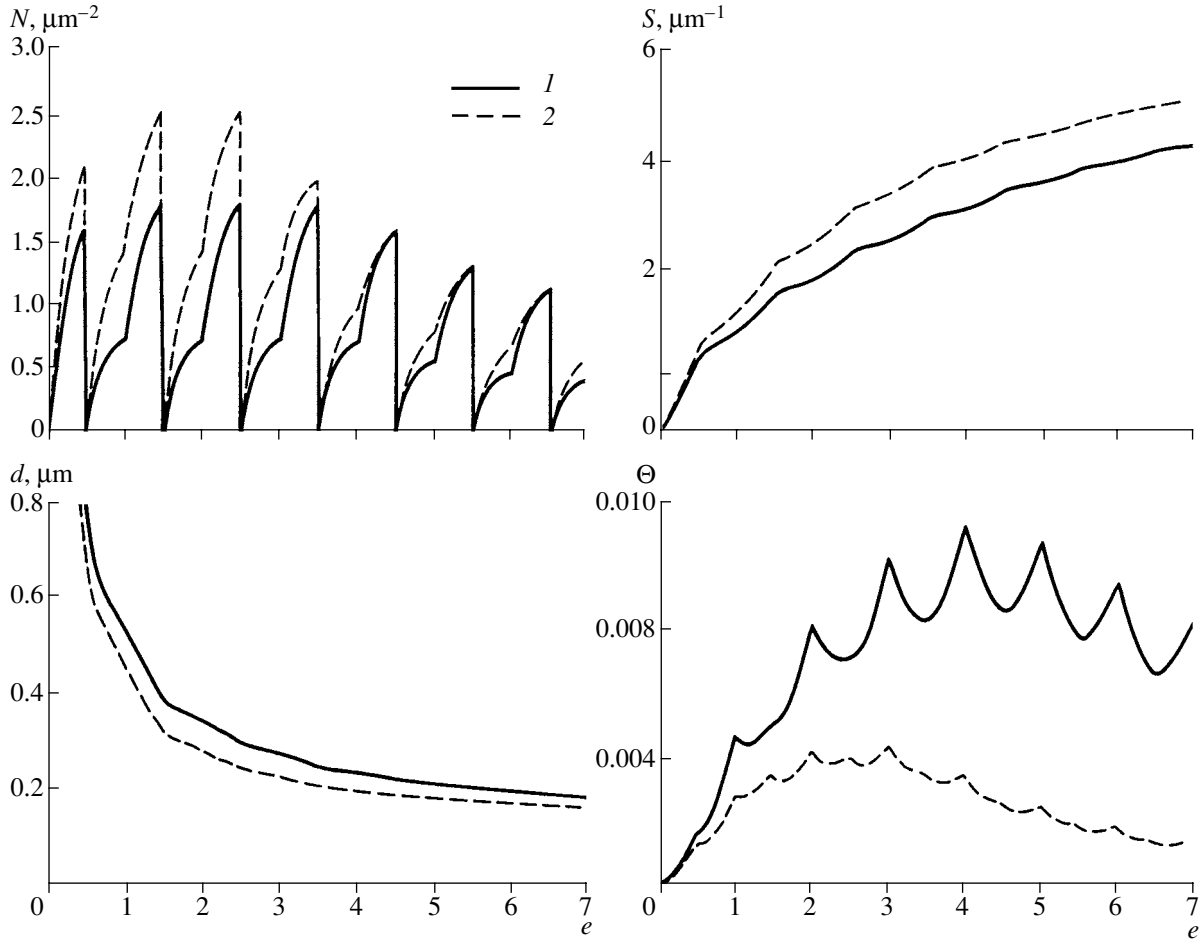

Fig. 6. Effect of a backpressure on the structural characteristics of grade 45 steel for TE realizing according to the scheme with dies having alternating unlike orientations: (*1*) seven twist dies without a backpressure and (*2*) seven twist dies with P_{bp} = 600 MPa.

often used in practice. Let us analyze these calculated curves.

The steplike character of the change in N, which is the number of AZs for SE, is explained by the form of Eq. (10). The gradual decrease in both curves in the $N(e)$ plot is caused by the formation of a significant fraction of fragments that do not undergo division. The activation of mutual sliding leads to a decrease in the intensity of internal-stress accumulation.

The $S(e)$ and $d(e)$ curves, which illustrate the grain refinement of the material structure, indicate that the grain refinement intensities of these treatments are virtually the same. In the case of DE, however, $e \approx 3$ is the practically achievable total strain at which a sample can still be considered as a bulk sample. Indeed, a blank diameter for DE is, as a rule, smaller than 50 mm. Then, at a logarithmic strain $e \approx 3$, the extrudate diameter is 10 mm, and extrudates produced at higher strains are hardly to be considered as bulk articles.

The curve of the relative porosity $\Theta(e)$ indicates that TE provides higher plasticity of a deformed material. As compared to DE, TE is a cyclic (substantially nonmonotonic) loading process, since the deformation direction changes within one pass inside a screw channel [16]. This process creates favorable conditions for microdiscontinuity healing in the material, which is illustrated by peaks in the porosity curve. Cyclic deformation results in higher plasticity of the deformed material; however, this is accompanied by its less intense grain refinement as compared to monotonic deformation. One of the methods to increase the intensity of substructure refinement during cyclic deformation is to increase its amplitude [5]. We will illustrate this thesis using TE as an example.

In Fig. 4, we compare two TE schemes, namely, a sequence of twist dies having the same orientation and a sequence of alternating dies oriented clockwise and counterclockwise. The difference in these two schemes consists in an increase in the deformation amplitude (Fig. 5).

In the case of the scheme with alternating unlike dies, dislocation charges do not relax from die to die; as a result, a larger number of AZs form and the $N(e)$ curve becomes higher. These excess AZs relax through the formation of additional high-angle boundaries and

through an increase in the porosity (see the $S(e)$ and $\Theta(e)$ curves, respectively). As was expected, we reached a certain improvement in the structural grain refinement but could not avoid an increase in the structural damage. As e increases, the detrimental effect of nonmonotonic deformation on the porosity decreases, and both $\Theta(e)$ curves merge at $e \geq 7$. Nevertheless, the gain in the length S of high-angle boundaries is retained.

A treatment that results in a significant decrease in the material plasticity should activate the formation of a fragmented structure when a pressure is applied. Figure 6 show the calculation results that reflect the role of a backpressure for TE according to the scheme with alternating unlike dies. It is clearly visible that the backpressure-induced increase in the pressure in the deformation zone leads to an increase in the grain refinement intensity, which is accompanied by a decrease in the porosity, i.e., by an increase in the material plasticity. It is obvious that, according to the structural characteristics considered in this work, this deformation scheme is optimal.

CONCLUSIONS

The simulation results demonstrate that TE is a more effective deformation accumulation scheme: it provides improved structural characteristics as compared to DE. The increase in the deformation amplitude in the case of the scheme with alternating unlike twist dies increases the grain refinement intensity; however, this is accompanied by an increase in the deformation-induced porosity and, hence, a decrease in the material plasticity. This problem can be solved by TE performed under pressure, which allows one to produce fine-grained materials with small damage.

REFERENCES

1. R. Z. Valiev and I. V. Aleksandrov, *Nanostructured Materials Produced by Severe Plastic Deformation* (Logos, Moscow, 2000) [in Russian].
2. R. Hill, *The Mathematical Theory of Plasticity* (Oxford University Press, Oxford, 1950; Gostekhteorizdat, Moscow, 1956).
3. V. A. Ogorodnikov, *Estimation of Metal Deformability during Metal Forming* (Vishcha Shkola, Kiev, 1983) [in Russian].
4. A. A. Bogatov, "On Metal Failure during Metal Forming," Kuznechno-Shtamp. Pr-vo, No. 8, 2–7 (1997).
5. V. L. Kolmogorov, V. A. Migachev, and V. G. Burdukovskii, "On the Construction of a Generally Accepted Phenomenological Theory for Failure during Plastic Deformation of Metals," Izv. Ross. Akad. Nauk, Ser. Met., No. 6, 133–141 (1995).
6. Y. Beygelzimer, "Grain Refinement versus Voids Accumulation during Severe Plastic Deformation of Polycrystal: Mathematical Simulation," Mech. Mater. **37**, 753–767 (2005).
7. H. J. Frost and M. F. Ashby, *Deformation Mechanism Maps* (Pergamon, Oxford, 1982).
8. Y. Y. Beygelzimer, B. M. Efros, V. N. Varukchin, and A. V. Khokhlov, "Continuum Model of the Structural-Inhomogeneous Porous Body and Its Application for the Study of Stability and Viscous Fracture of Materials Deformed under Pressure," Eng. Fract. Mech. **48** (5), 629–640 (1994).
9. P. G. Cheremskoi, V. V. Slezov, and V. I. Betekhtin, *Pores in Solids* (Energoatomizdat, Moscow, 1990) [in Russian].
10. V. V. Rybin, *Severe Plastic Deformation and Metal Fracture* (Metallurgiya, Moscow, 1986) [in Russian].
11. A. N. Kolmogorov, "On the Logarithmically Normal Size Distribution of Particles during Crushing," Dokl. Akad. Nauk SSSR **31**, 99–101 (1941).
12. A. S. Kao, H. A. Kuhn, O. Richmond, et al., "Tensile Fracture and Fractographic Analysis of 1045 Spheroidized Steel under Hydrostatic Pressure," J. Mater. Res. **5** (1), 83–91 (1990).
13. V. V. Rybin, "Structural–Kinetic Aspects of the Physics of Developed Plastic Deformation," Izv. Vyssh. Uchebn. Zaved., Fiz., No. 3, 7–22 (1991).
14. V. Segal, "Severe Plastic Deformation: Simple Shear versus Pure Shear," Mater, Sci. Eng., Ser. A **338**, 331–344 (2002).
15. Ya. E. Beigel'zimer, V. N. Varyukhin, and B. M. Efros, *Physical Mechanics of Hydrostatic Treatment of Materials* (DonFTI NANU, Donetsk, 2000) [in Russian].
16. Ya. E. Beigel'zimer, V. N. Varyukhin, D. V. Orlov, and S. G. Synkov, *Twist Extrusion—Deformation Accumulation Process* (TEAN, Donetsk, 2003) [in Russian].